SAND2013-3472C

A Discrete Error Transport Equation Error Source Model for Mesh Adaptation

Nicholas G. Currier* and Kenneth J. Franko†

Sandia National Laboratories, Albuquerque, NM 87185-1124

Computational fluid dynamics (CFD) is a powerful analysis tool for engineering analysis of aerodynamic devices. Though great effort has been expended to assist the CFD practitioner in mesh generation efforts, investigation of spatial discretization error is still one of the primary time costs associated with field simulations. As complexity in both physics and geometry continues to increase, uniform grid refinement studies are not always practical from either a time or computational cost perspective. Error transport equations have been investigated by many researchers in recent years with the goal of providing greater confidence in simulation results while utilizing only a single mesh. One of the primary difficulties in applying these methods is the computation of a reliable error source model. This work presents a method for approximating these error sources with the intent of creating a general model which is applicable to all flux types within a general gas dynamics framework. Adaptivity results as well as comparison with a popular error source model are presented.

Nomenclature

Q	Conservative variable vector
Q_H^{HO}	MUSCL extrapolated conservative variable vector
Q_H^{LO}	Piecewise continuous conservative variable vector
A	Flux Jacobian
$\lvert\tilde{A}\rvert$	Flux Jacobian evaluated at Roe averaged state
R	Error source
q	Primitive variable vector $[u, v, w, T]^T$
F	Flux vector
$\hat{\vec{n}}$	Normalized face area vector
V	Volume
ϵ	Computed error
θ	Covariant velocity $[\hat{n}_x u + \hat{n}_y v + \hat{n}_z w]$

I. Introduction

In recent years, computational fluid dynamics (CFD) has become an increasingly important tool in engineering portfolios. The ability to simulate fluid physics on complex configurations with a relatively short time table is invaluable in engineering practice. However, one of the primary shortcomings of CFD is the inability to reliably and robustly predict error in simulation results. In particular, the error related to spatial discretization is notoriously hard to estimate *a posteriori*. Richardson's extrapolation[1] has been utilized to great effect but is either impractical or insufficient in many cases. The cost associated with these uniform grid refinement studies is often too high and non-monotone behavior renders the method unusable. Richardson's extrapolation is also not practical for error estimation in time-accurate studies with evolving flow features.

*Graduate Student Intern, Computational Thermal & Fluid Mechanics, Mail Stop 0828, AIAA Member.
†Member of Technical Staff, Computational Thermal & Fluid Mechanics, Mail Stop 0828, AIAA Member.

Discrete error transport equations compute error estimation based on the concept that error is generated due to local defects in mesh resolution and propagated along relevant physical characteristics. It has been shown in other work that error can be predicted very accurately given the correct estimation of these error sources. While Richardson's extrapolation has been used to compute these sources exactly,[2] this method is impractical for the same reasons discussed above .

Much research has been performed to develop models for this source term and several useful techniques have been developed as a result. Zhang *et al*[3] developed a model based on a finite difference modified equation analysis which was adapted by Cavallo[4] for use in general element unstructured finite volume schemes. This model in particular has shown great utility for practical problems. However, this model is developed specifically for the numerical scheme given, namely Roe's flux.[5] Williams also investigated an error source model based on uniform grid refinement and a model based on higher order polynomial solution fits.[2] These ideas are also common in adjoint based error estimation for determining defects in residual calculations.[6,7]

In addition, it has been shown in literature that feature based adaptation methods are lacking in some critical aspects. In particular, feature based adaptation often cannot capture flow features which were not present in the coarse mesh solution. Other work has shown excellent performance of adjoint based error indicators.[7–9] The added expense of adjoint computation, however, makes these methods less desirable for adaptation.

In this work simulations performed within the Sandia National Labs' code SIERRA Gas Dynamics module Conchas are shown. We present an error source model with the intent of developing a useful error indicator for *in situ* mesh adaptation. Providing rigorous error bounds on the computed solution was not an objective here but the method compares favorably with previously reported models. Both one-dimensional and two-dimensional validation cases are shown as well as a results for a thoroughly studied three-dimensional validation case.

II. Governing Equations

The governing equations considered here are the three-dimensional Euler equations. The Euler equations can be written in continuous integral (conservation) form as

$$\frac{\partial}{\partial t}\int_{\Omega} Q\, d\mathcal{V} + \int_{\partial\Omega} F(Q)\cdot\hat{\vec{n}}\, dA = 0 \tag{1}$$

where the solution vector, Q, and the flux vector, F are

$$Q = \begin{bmatrix} \rho \\ \rho u \\ \rho v \\ \rho w \\ \rho e_t \end{bmatrix} \tag{2}$$

$$F(Q)\cdot\hat{\vec{n}} = \begin{bmatrix} \rho\theta \\ \rho u\theta + P\hat{n}_x \\ \rho v\theta + P\hat{n}_y \\ \rho w\theta + P\hat{n}_z \\ \rho h_t\theta \end{bmatrix} \tag{3}$$

and θ is defined as

$$\theta = \hat{n_x}u + \hat{n_y}v + \hat{n_z}w \tag{4}$$

III. Error Transport Equation

The Euler equations can also be written for a discrete PDE where Q_H denotes a discrete solution on some finite space.

$$\frac{\partial}{\partial t}\int_{\Omega} Q_H\, d\mathcal{V} + \int_{\partial\Omega} F(Q_H)\cdot\hat{\vec{n}}\, dA = \int_{\Omega} R(Q_H)\, d\mathcal{V} \tag{5}$$

$R(Q_H)$ is the residual deviation of the discrete solution from that of the continuous PDE. Subtracting Equation 5 from Equation 1 results in the following expression

$$\frac{\partial}{\partial t}\int_\Omega (Q - Q_H)\, d\mathcal{V} + \int_{\partial\Omega} F(Q) - F(Q_H)\cdot \hat{\vec{n}}\, dA = -\int_\Omega R(Q_H)\, d\mathcal{V} \tag{6}$$

Taking advantage of the homogeneous property of the flux function we can rewrite $F(Q) - F(Q_H)$ as $A(Q, Q_H)(Q - Q_H)$. Since the exact solution is not known *a priori* we can reasonably replace $A(Q, Q_H)$ with the Jacobian computed for each face on the discrete mesh, $A(Q_H)$. This is also convenient because in our implicit flow solver these values are required for solution and are thus available cheaply. We define the solution error to be $\epsilon = Q - Q_H$. Rewriting Equation 6 using these given definitions gives

$$\frac{\partial}{\partial t}\int_\Omega \epsilon\, d\mathcal{V} + \int_{\partial\Omega} A(Q_H)\epsilon\cdot \hat{\vec{n}}\, dA = -\int_\Omega R(Q_H)\, d\mathcal{V} \tag{7}$$

which is the discrete error transport equation.

III.A. Error Source Models

The right hand side of Equation 7 is referred to here as the error source. Given appropriate monotone solution behavior and several uniformly refined grids, this term can be computed to arbitrary accuracy as was done by Williams.[2] However, for real geometries of engineering interest, it is often quite expensive to perform even one level of uniform refinement for grid convergence studies. Performing multiple levels of uniform refinement in three-dimensional, complex geometries is certainly not possible when the original problem already stretches the limits of computing capacity. In addition, if the solution can be obtained to arbitrary accuracy in this manner, there is simply no need for the solution of the error transport equations. Thus, we require a method of evaluating the error source which is efficient as well as providing reasonable estimates for error generation based on grid defects.

III.B. Roe's Flux Based Dissipation Model

Zhang *et al*[3] developed a model for the error source based on a modified equation developed for a one-dimensional explicit finite-volume discretization. This discretization can be written pointwise as

$$Q_i^{n+1} = Q_i^n - \frac{\Delta t}{\Delta x}(F_{i+1/2}^n - F_{i-1/2}^n) \tag{8}$$

where i and n represent the control volume and time level respectively. The values $F_{i\pm1/2}^n$ represent the flux values at the two faces of the one-dimensional control volumes. Roe's flux at each face can be written as a combination of a central and upwinded part. For example, at the right and left faces we have

$$F_{i+1/2}^n = \frac{1}{2}(F_{i+1}^n + F_i^n) - \frac{1}{2}|\tilde{A}_{i+1/2}^n|\,\Delta Q_{i+1/2} \tag{9}$$

$$F_{i-1/2}^n = \frac{1}{2}(F_i^n + F_{i-1}^n) - \frac{1}{2}|\tilde{A}_{i-1/2}^n|\,\Delta Q_{i-1/2} \tag{10}$$

where $\Delta Q_{i+1/2} = Q_{i+1} - Q_i$ and $\Delta Q_{i-1/2} = Q_i - Q_{i-1}$. The $\tilde{A}$ denotes the flux Jacobian evaluated at the Roe averaged state of a control volume face.

The derivation of the modified equation for this explicit scheme is straight forward with the result being

$$\begin{aligned}\frac{\partial Q}{\partial t} + \frac{\partial F}{\partial x} = &-\frac{1}{2\Delta x}(\,|\tilde{A}_{i+1/2}|(Q_{i+1} - Q_i) - |\tilde{A}_{i-1/2}|(Q_i - Q_{i-1})\,) \\ &-\frac{\Delta t}{2}\frac{\partial^2 Q}{\partial t^2} - \frac{\Delta x^2}{6}\frac{\partial^3 F}{\partial x^3} - \frac{\Delta t^2}{6}\frac{\partial^3 Q}{\partial t^3} + O(\Delta x^3, \Delta t^3)\end{aligned} \tag{11}$$

Zhang *et al* suggest utilizing the leading terms of this truncation error analysis as the basis for computing the error source. Cavallo extended this to general unstructured grids by defining the error source as the sum of the upwinded flux contributions across all adjacent control volume faces. That is

$$R_i(Q_H) = -\frac{1}{2V_i}\sum_{j=1}^{Nfaces}(|\tilde{A}_j|\,\Delta Q_j)\cdot\vec{n} \tag{12}$$

where $\Delta Q_j = Q_{L,j} - Q_{R,j}$. The values of the conserved variables at the left and right of a given face j are $Q_{L,j}$ and $Q_{R,j}$ respectively. Note here that $\vec{n}$ is the un-normalized directed face area vector.

III.C. MUSCL Extrapolated Flux Model

The MUSCL extrapolated flux model was developed based on the conceptual premise that regions of high gradient are likely sources of error. Feature based adaptation methods would refine strictly based on these local gradient values. However, this practice does not incorporate the nonlinearities present within the local flux evaluation. By instead looking at the difference between a MUSCL extrapolated flux[10] and a flux evaluated as piecewise continuous within a control volume, the high gradient regions which drive grid defect based errors become much easier to identify.

Flow variables are extrapolated to each control volume face via the use of a field gradient. The variables at these faces are computed by

$$Q^{HO} = Q + \nabla Q \cdot \vec{r} \tag{13}$$

where $\vec{r}$ is the position vector constructed from the control volume centroid to the face centroid. Here, the higher order face values are denoted Q^{HO} and likewise, the piecewise constant variables are Q^{LO}. In the SIERRA code, the non-conserved primitives are extrapolated to the face of each control volume and the conservative fluxes are reconstructed from these.

Our error source construction looks like

$$R_i(Q_H) = \frac{1}{V_i} \int_{\partial\Omega} (F(Q_H)^{HO} - F(Q_H)^{LO}) \cdot \hat{\vec{n}}\, dA \tag{14}$$

Notice that this expression can also be expanded by the homogeneous property of the flux like

$$F(Q_H^{HO}) - F(Q_H^{LO}) = A(Q_H^{HO}, Q_H^{LO})\,(Q_H^{HO} - Q_H^{LO}) \tag{15}$$

Since most flow solvers do not require nor compute the Jacobian matrix with MUSCL extrapolated flow variables, it is convenient to approximate this as

$$A(Q_H^{HO}, Q_H^{LO})\,(Q_H^{HO} - Q_H^{LO}) \approx A(Q_H^{LO})\,(Q_H^{HO} - Q_H^{LO}) \tag{16}$$

Thus, our error source term can be re-expressed as

$$R_i(Q_H) = \frac{1}{V_i} \int_{\partial\Omega} A(Q_H^{LO})\,(Q_H^{HO} - Q_H^{LO}) \cdot \hat{\vec{n}}\, dA \tag{17}$$

This evaluation requires $\sim O(n^2)$ operations per edge which, when compared to the literal implementation of Roe's flux involving two matrix vector multiplications, is roughly half as expensive. If a one-sided Roe's flux or other less expensive flux implementation were utilized this cost savings will not likely be as substantial. This approximation was not used here as the desire to generalize the error source model to other flux types as they become available was deemed more beneficial.

Contrary to the method of computing the error source of Zhang *et al* this method is fully applicable to many different flux formulations without need for modification. Also, worth note is that this model is applicable to error sources which may arise from the discretization of viscous contributions. For computation of viscous contributions, the gradients of velocity and temperature are required. We refer to these primitive variables as q here.

$$q = \begin{bmatrix} u \\ v \\ w \\ T \end{bmatrix} \tag{18}$$

If a directional method is utilized to extrapolate a "higher-order" gradient to the face centroid locations as was done by Hyams,[11] neglecting the directional correction will also result in a change in approximate gradient. These higher and lower order gradient evaluations at a control volume face are

$$(\nabla q)^{HO} = \frac{1}{2}(\nabla q_L + \nabla q_R) + [q_R - q_L - \frac{1}{2}(\nabla q_L + \nabla q_R) \cdot \vec{\Delta s}] \frac{\vec{\Delta s}}{|\vec{\Delta s}|^2} \tag{19}$$

$$(\nabla q)^{LO} = \frac{1}{2}(\nabla q_L + \nabla q_R) \tag{20}$$

Integrating the difference between the viscous fluxes based on these reconstructed gradients will result in a residual defect based on the mesh discretization. This has not yet been implemented and future tests will evaluate the performance of this method for viscous error sources.

III.D. Boundary Conditions

Several different approaches have been taken to boundary conditions in literature. Williams[2] derives boundary conditions for the error transport equations based on the boundary condition applied at each surface. This approach seems to be the most thorough treatment of boundary conditions undertaken. Cavallo[4] utilizes zero boundary conditions on inflow boundaries, where presumably error has not been generated, and extrapolation conditions elsewhere. Ilinca *et al*[12] advocate the formation of boundary conditions based on the characteristics of both the inviscid and viscous flux function linearizations. However, this method requires the eigen-decomposition of these fluxes depending on the flux implementation.

The code presented here utilizes zero boundary conditions on inflow boundaries, reflected velocity boundary conditions on inviscid surfaces, and extrapolation boundary conditions elsewhere. It was found that for the ramp case, the symmetry boundary conditions were necessary to predict the propagation of error along the ramp. Though these boundary conditions are non-consistent with the flowfield boundary conditions, no undesired effects on stability were observed. It is expected that the extrapolated boundary condition will be reflective should boundaries be placed too close to immersed bodies. It is unknown what effect this might have on computed error bounds. However, it is common to place farfield boundaries at many body lengths away as standard practice. This mostly mitigates concern about reflectivity.

IV. Results

IV.A. 2D Supersonic Ramp

A standard compressible fluid dynamics test case was utilized for comparison and validation of the two error source models presented here. A two-dimensional ramp with a half-angle of 15 degrees was simulated with a freestream pressure 287.14 Pa and temperature of 250.35 K. A freestream flow of Mach 1.9 impinges on the ramp and a crisp, oblique shock forms at an angle of 51.3 degrees.

The solution to this problem is demonstrated on two meshes. The first mesh is quite coarse with 40 control volumes in each of the coordinate directions.This mesh was used for computing the solution to the error transport equations. The second mesh is used as the validation solution and has 250 control volumes in each direction. Figure 1 shows the comparison of density for these two meshes. Both solutions are shown with a second order MUSCL extrapolation and a Venkatakrishnan limiter.[13]

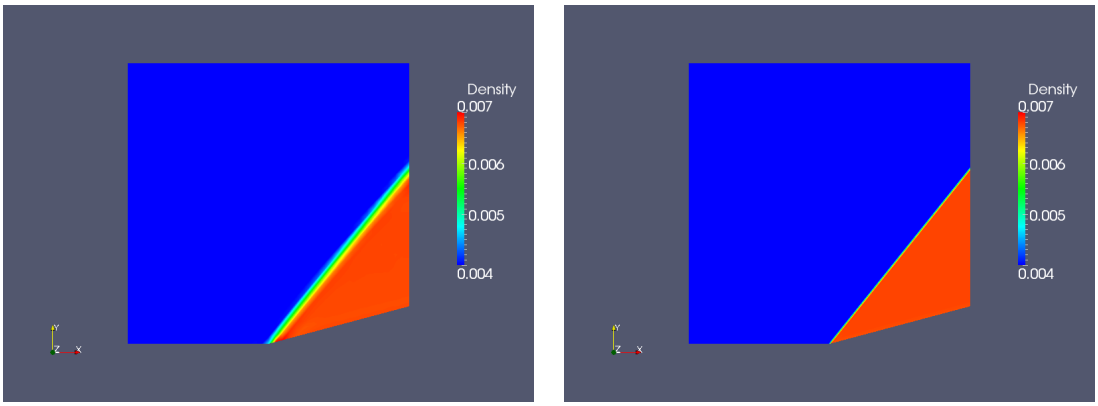

(a) Density solution on 40x40 mesh (b) Density solution on 250x250 mesh

Figure 1. Comparison of density on both the coarse and fine "exact" meshes

Both the dissipation and MUSCL extrapolation error source models were used to compute the error via the error transport equations. Both the error sources and the solution to the error transport equations

were computed using first order spatial discretization. This practice leads to more dissipative computed error and thus more conservative predicted errors. Tong and Luke[14] report that for the same test case, the computed error does not contain the magnitude of the actual error. Here, this is not the case. Using the first order spatial discretization shows that both methods span the actual error. However, the computed error in the dissipation based model case is nearly twice the actual error. The maximum magnitude of computed error in this case is 2.4E-3. Figure 2 is shown with the magnitude clipped for comparison purposes. The extrapolation method does not overpredict the error nearly as much and shows a maximum magnitude in error of 1.1E-3. The actual error maximum is 9.4E-4. In this case it seems that the extrapolation error source approximation predicts the error more closely than the dissipation model. Figure 2 shows only error in density. Error in other variables is qualitatively similar for other variables.

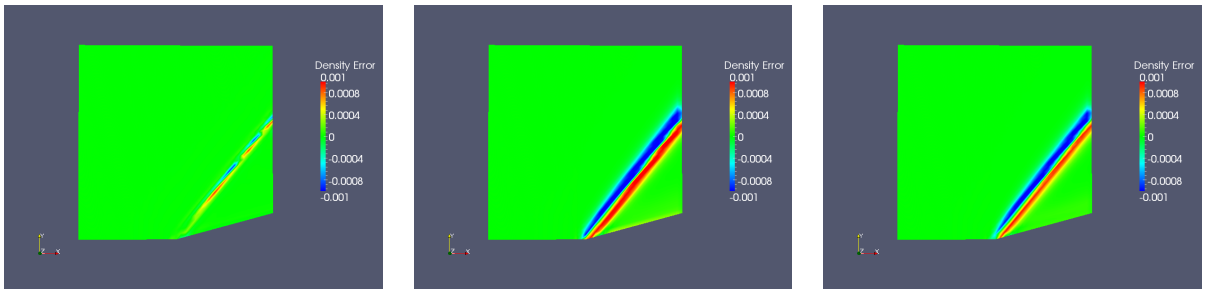

(a) Actual error in density

(b) Computed error using dissipation error source

(c) Computed error using MUSCL extrapolation error source

Figure 2. Comparison of extrapolated error with that computed via the two error source methods

IV.B. Transonic Onera M6 Wing

A simulation of a three-dimensional transonic Onera M6 wing was performed at a Mach number of 0.8395 and an angle of attack of 3.06 degrees. Experimental data is available for these conditions,[15] though no direct comparisons are made here. Figure 3 shows the density solution for the top side of the airfoil. The "lambda" shock structure is clearly visible. Balasubramanian and Newman show in their work[7] that this shock structure is not visible on poorly resolved meshes.

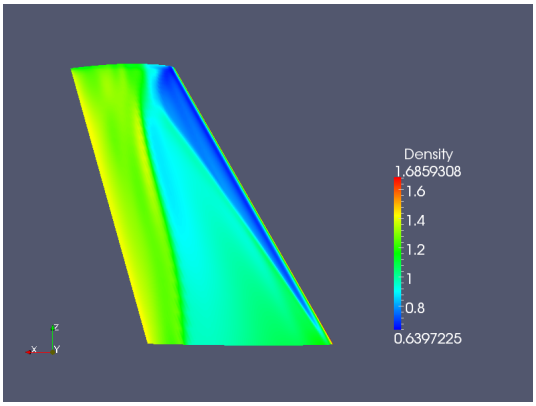

Figure 3. Density solution for Onera M6 wing

Of particular interest for this test case are differences predicted error between both the dissipation and extrapolation error source models. Figure 4 shows predicted error in density at steady-state on the top surface of the wing for both error source models.

Again, it is clear that the dissipation error source predicts a greater magnitude of error near the shock location. The maximum magnitude of error predicted by the dissipation error source model is near the wingtip trailing edge. It is an order of magnitude greater than any error predicted by the extrapolation error source. This computed error is also three times the maximum value of density computed on the airfoil surface. It is suspected that this is unphysical and the result of an overshoot caused by difficulty in the

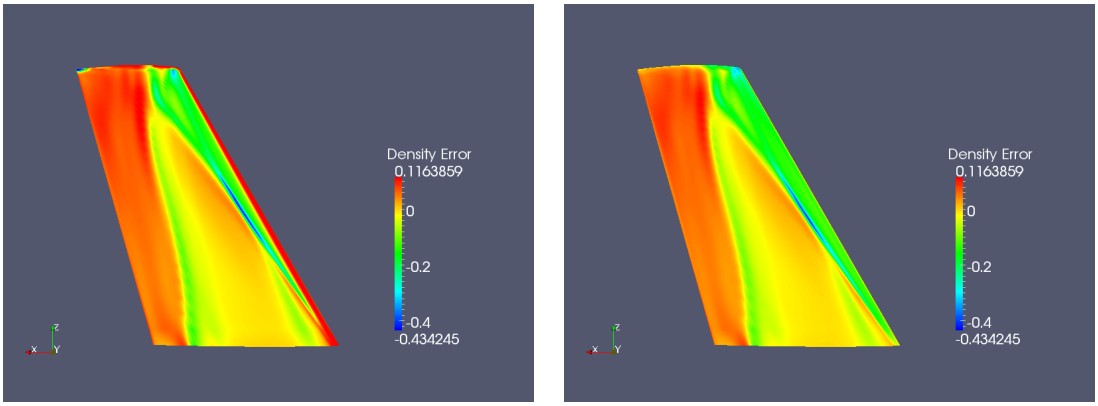

(a) Density error computed with dissipative error source

(b) Density error computed with MUSCL extrapolation error source

Figure 4. Comparison of computed density error for two error source models

evaluation of derivatives near the relatively coarse wingtip. The error source in the ρw term is also quite high in this location for the dissipation based model. Celik *et al*[16] also noted difficulty with the error source for error transport equations in the vicinity of sharp gradients. They advocate the addition of diffusion terms to the error transport equations. They also report an increase in accuracy in the computed error as a side effect of the addition of these terms. This might be expected considering the error transport equations do not contain diffusive terms in the present formulation. Cavallo shows in his work[4] that for viscous simulation of shear dominated flows the predicted error bars do not contain the true solution. This again would suggest that diffusion terms should be included in the computation of the error solution.

V. Error Transport Equations for Adaptation

With the goal of developing a mesh adaptation indicator for fully turbulent, unsteady flows, there are several criterion which must be met. Foremost, the indicator must be computed at relatively low expense. For simulations where uniform refinement studies are not currently possible due to problem size, this would be a disruptive technology. In this respect, computing solution to the error transport equations certainly are within reason. In three-dimensions, the number of grid points and thus cost is expected to increase for uniform refinement studies as a factor of eight. For example, a 500x500x500 mesh (125 million volumes) which is uniformly refined will result in a mesh of 1 billion volumes. In this case, the problem size is certainly beyond the capabilities of all but the most capable machines today. If a reasonable bound on local error can be obtained in less than the factor of eight increase, confidence on large problems can be greatly increased. The error transport equation implementation shown here results in approximately 60% increase in total computation cost when computed at every timestep. This suggests the cost if used for unsteady simulations. If computed for a steady-state solution the additional cost is nearly the same as one additional solver iteration. This is certainly very reasonable.

Secondly, the indicator must be at least as robust as the core solver. This issue deserves a more thorough investigation. From the numerical results presented here, it appears that the dissipation based error source model suffers from possible stability issues with regards to overshoots and undershoots near discontinuities. For the an error source model to be applied to transonic and hypersonic problems, stability near shocks is a requirement.

Finally, the indicator must be capable of refining in regions which are non-obvious to the CFD practitioner. The work of Zhang *et al*[3] suggests that refining at the error location itself is of little value. Since error propagates along characteristic directions in hyperbolic problems, the error solution itself has little value in terms of the identification of local grid defects. Zhang showed that refining in the locations of greatest error source shows large reduction in overall solution error. In their work, refining based on greatest local error showed little improvement in solution quality. However, Zhang presented only one-dimensional test problems. It is unclear whether this conclusion also extends to two and three dimensions. If this assumption does hold, there is the issue of how to associate error source locations with output functionals of engineering

interest. This is one of the primary shortcomings of the solution of error transport equations when compared to adjoint based error estimation methods. Cavallo[4] suggested a method for the estimation of error in functional outputs. However, it is unclear whether this methodology can be extended to relate error in a particular output to the source of this error in the field. Clearly more investigation into this issue is warranted.

VI. Adaptation Test case

A test case for adaptive refinement within SIERRA was formulated based on a cylinder in Mach 1.5 crossflow. Conditions for the farfield were set at standard temperature and pressure. This test case results in the formation of a bow shock. The location of this bow shock is highly dependent on mesh resolution as well as thermochemistry in the flowfield. For this simulation, ideal gas assumptions were made and no thermochemistry was present.

Three meshes were examined. The first mesh was used as a baseline solution and is considered unrealistically fine for engineering purposes. This mesh consists of 81,929 nodes. The second mesh is considered under resolved. It was used as a baseline mesh for refinement based on the computed error in density from the error transport equations. The third mesh was refined based on an a statistical measure of computed error in density. The mesh was refined in regions where the magnitude of error was greater than two standard deviations above the mean and coarsened where the error was below one standard deviation above the mean. The resulting mesh should, in theory, result in equidistribution of error in the solution field. The error source used was the extrapolated MUSCL method.

Figure 5 shows the density solution on the three meshes. The error equations were allowed to evolve with the flow field solution and adaptivity (both refinement and coarsening) was allowed at every iteration. Minimum cell size was fixed to prevent excessive localized differences in control volume size near the shock. The black contour line shown in Figure 5 is fitted to the shock location of the fine mesh for comparison purposes. Though the shock location is not predicted perfectly it must be noted that even the refined mesh has approximately 75% fewer nodes, and therefore expense, when compared to the finest mesh.

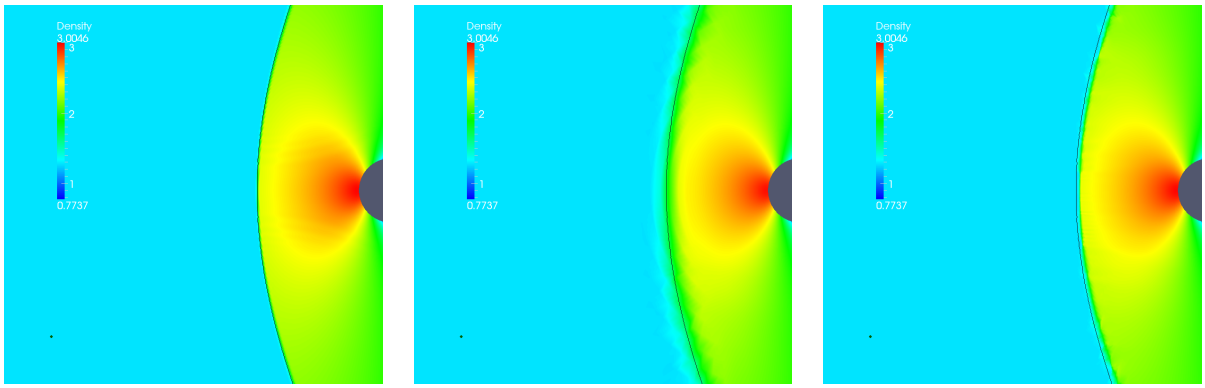

(a) Density computed on 81,929 node mesh

(b) Density computed on 5,000 node mesh - Unrefined

(c) Density computed on 21,932 node mesh - Adaptively refined

Figure 5. Comparison of meshes utilized for solution

Figure 6 shows the density error computed on the coarse mesh with no refinement. Clearly the shock location is spanned by the computed error. However, the location is not predicted perfectly. It is suspected that by computing the error transport equation solution with a first order spatial method the ability to precisely resolve discontinuities is lost.

The three meshes which were utilized in the adaptivity investigation are shown in Figure 7. Clustering of mesh points behind the "exact" shock location is believed to be a result of the lower order spatial method used to compute the solution error. Further work to extend the method to second order spatial accuracy should provide evidence clarifying this deficiency.

Table 1 shows the L2 norm of the actual error of the solution in density when compared to the solution on the finest mesh. As might be expected, the error norm is reduced drastically on the refined mesh. The norm of the error on the refined mesh is approximately 36% of the same norm computed on the coarse mesh.

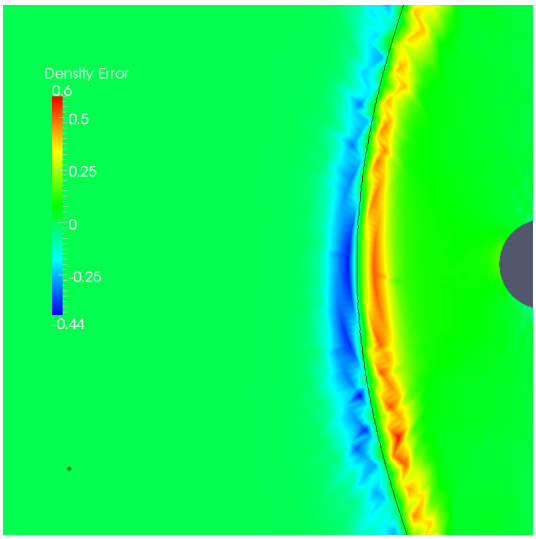

Figure 6. Computed density error with MUSCL extrapolated error source on coarse mesh

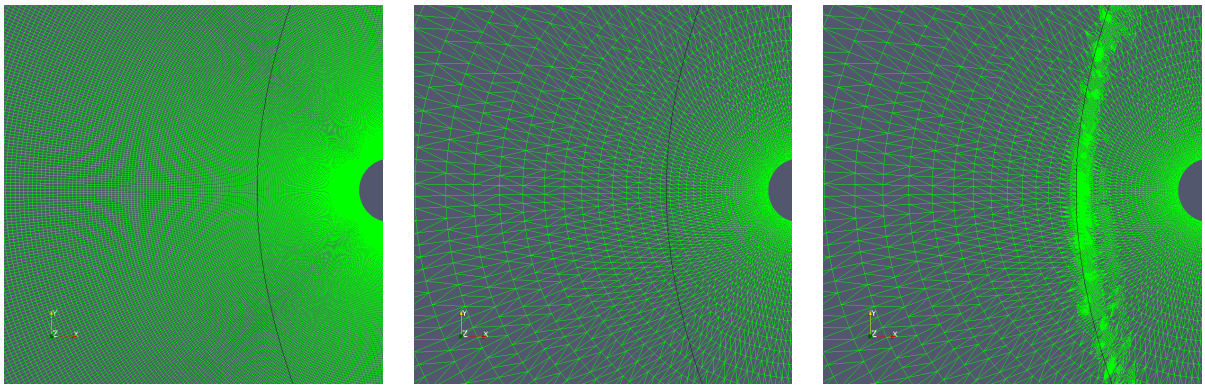

(a) "Exact" 81,929 node mesh (b) Unrefined 5,000 node mesh (c) Adaptively refined 21,932 node mesh

Figure 7. Comparison of meshes utilized for solution

Table 1. Comparison of the L2 norm of error pre and post refinement

	Number of nodes	$\|\text{Actual Error}\|_2$
Fine Mesh	81,929	–
Coarse Mesh	5,000	.07217
Refined Mesh	21,932	.02607

Both solutions were converged until a reduction in residuals was no longer achieved. It is worth noting that the flux limiter was much more ill-behaved in the adapted case. This hindered the ability to obtain deep solution convergence. This is suspected to be related to grid quality and work is currently underway to improve cell quality during the refinement process.

VII. Conclusion

A new error source model for general flux types has been investigated for the discrete error transport equations. The error source is based on the surface integrated difference between extrapolated higher and lower order fluxes for generalized unstructured meshes.

The new method compares favorably to a method which has previously gained favor in literature. Several test problems are examined to highlight qualitative differences in the methods. Also, a full adaptivity study is performed on a common hypersonic test problem. Bow shock location is predicted reliably with far less expense than for the benchmark solution. The new error source method combined with solution of the error transport equations has shown promise in the implementation of *in situ* mesh adaptivity to the Sandia National Labs' SIERRA Gas Dynamics module Conchas.

Future work will include re-investigation of these methods with a second order accurate solution to the error transport equations. It is expected the higher spatial order of accuracy will provide enhanced prediction of discontinuity locations within the solver. Also, future studies will include demonstration of *in situ* mesh adaptation for unsteady gas dynamics simulations.

Acknowledgments

Sandia National Laboratories is a multi-program laboratory managed and operated by Sandia Corporation, a wholly owned subsidiary of Lockheed Martin Corporation, for the U.S. Department of Energy's National Nuclear Security Administration under contract DE-AC04-94AL85000.

References

[1]Richardson, L. F., "The Approximate Arithmetical Solution by Finite-Differences of Physical Problems Including Differential Equations, with an Application to the Stresses in a Masonry Dam," *Philosophical Transactions of the Royal Society of London, Series A*, Vol. 210, 1910, pp. 307–357.

[2]Williams, B., *Estimation of Grid-Induced Errors in Computational Fluid Dynamics Solutions Using a Discrete Error Transport Equation*, Ph.D. thesis, Iowa State University, 2009.

[3]Zhang, X. D., Trépanier, J.-Y., and Camarero, R., "A Posteriori Error Estimation for Finite-Volume Solutions of Hyperbolic Conservation Laws," *Computer Methods in Applied Mechanics and Engineering*, Vol. 185, 2000, pp. 1–19.

[4]Cavallo, P. A. and Sinha, N., "An Error Transport Equation with Practical Applications," *18th AIAA Computational Fluid Dynamics Conference*, 2007.

[5]Roe, P. L., "Characteristic-based Schemes for the Euler Equations," *Annual Review of Fluid Mechanics*, Vol. 18, 1986, pp. 337–365.

[6]Balasubramanian, R., *Error Estimation and Grid Adaptation for Functional Outputs Using Discrete-Adjoint Sensitivity Analysis*, Ph.D. thesis, Mississippi State University, 2002.

[7]Balasubramanian, R. and Newman III, J. C., "Comparison of Adjoint-Based and Feature-Based Grid Adaptation for Functional Outputs," *International Journal for Numerical Methods in Fluids*, Vol. 53, 2006, pp. 1541–1569.

[8]Fidkowski, K. J. and Darmofal, D. L., "Review of Output-Based Error Estimation and Mesh Adaptation in Computational Fluid Dynamics," *AIAA Journal*, Vol. 49, 2011, pp. 673–694.

[9]Dwight, R. P., "Efficient A Posteriori Error Estimation for Finite Volume Methods," Tech. rep., NATO Research and Technology Organization, 2007.

[10]Van Leer, B., "Towards the Ultimate Conservative Difference Scheme. V. A Second-Order Sequel to Godunov's Method," *Journal of Computational Physics*, Vol. 32, 1979, pp. 101–136.

[11]Hyams, D. G., *An Invetigation of Parallel Implicit Solution Algorithms for Incompressible Flows on Unstructured Topologies*, Ph.D. thesis, Mississippi State University, 2000.

[12]Ilinca, C., Zhang, X. D., Trépanier, J.-Y., and Camarero, R., "A Comparison of Three Error Estimation Techniques for Finite-Volume Solutions of Compressible Flows," *Computer Methods in Applied Mechanics and Engineering*, Vol. 189, 2000, pp. 1277–1294.

[13]Venkatakrishnan, V., "On the Accuracy of Limiters and Convergence to Steady-State Solutions," *31st AIAA Aeropace Sciences Meeting and Exhibit*, 1993.

[14]Tong, X.-L. and Luke, E. A., "An Error Transport Equation in Primitive Variable Formulation," *49th AIAA Aerospace Sciences Meeting and Exhibit*, 2011.

[15]Schmitt, V. and Charpin, F., "Pressure Distributions on the ONERA-M6 Wing at Transonic Mach Numbers," Tech. Rep. AGARD AR 138, Report of the Fluid Dynamics Panel Working Group, May 1979.

[16]Celik, I., Hu, G., and Jr., A. B., "Further Refinement and Bench Marking of a Single-Grid Error Estimation Technique," *41st AIAA Aerospace Sciences Meeting and Exhibit*, 2003.